A Passivity-Based Controller for Power Management of a Fuel Cell System

M. HILAIRET, O. BETHOUX, T. AZIB, R. TALJ
Laboratoire de Génie Electrique de Paris (LGEP) / SPEE-Labs, CNRS UMR 8507;
SUPELEC; Université Pierre et Marie Curie P6; Université Paris-Sud 11;
11 rue Curie, Plateau de Moulon F91192 Gif sur Yvette CEDEX
mickael.hilairet@lgep.supelec.fr, olivier.bethoux@lgep.supelec.fr

***Abstract*— The problem of power management of a fuel cell system involving a hydrogen fuel cell with supercapacitors for applications with high instantaneous dynamic power is adressed in this paper. The problem is solved using a non-linear controller. The design of the controller is based on the interconnection and damping assignment - passivity based control. To prove the global stability and boundednes of the system, we exploit the well-known passivity properties. The stability properties, the number of degree of freedom and performances of the controller is discussed.**

***Index Terms*— Fuel cell, supercapacitors, energy management, energy-shaping, port-controlled Hamiltonian systems, IDA-PBC methodology.**

I. INTRODUCTION

To comply with environmental norms, development of electric and hybrid vehicles is increasing since 2009. In this context, the development of fuel cell (FC) system based on proton exchange membrane as the main energy source is considered. The combination of hydrogen and FC can increase the power and driving range of the vehicles. However, to ensure a good health of the FC, it is necessary that the FC delivers a slowly varying current, no more than 4A/s for a FC 0.5kW/12.5V [1], and 10A/s for a FC of 20kW/48V [2].

Thus, FC needs to be associated with other sources which provide the short pulse energy and make up for the temporary failure of FC. Nowadays, these auxiliary sources can be either batteries or supercapacitors (SCs). But thermal constraints in automotive applications are severe and the braking power requested is even greater than the accelerating power. Sometimes batteries are not able to support this high power charge and the discharge conditions, whereas supercapacitors can operate even at low temperatures (e.g. -20°C), and are already industrially manufactured. Therefore, for fast car power demands, supercapacitors are probably the best suited components. At that point, the design challenge is to choose power components, to design an adapted architecture and also to define the appropriate associated control strategy.

In this article, we consider the practically important, and theoretically chanllengyng problem of power management of an hydrogen FC system assited by a reversible impulse energy source (the supercapacitors). Several electric architectures of the hybrid system exist and can be classified into three categories : series, cascaded and parallel. The literature has shown that the parallel architecture is the most advantageous structure : it has lower component stresses, easiness power management and a higher reliability. Three topologies of parallel structures for the hybrid power FC/SCs can be distinguished. The three major objectives of this hybridization are the dynamics respect of the FC (mainly limited by the time response of the air compressor), the control of the storage device (SCs) state of charge and the power response (positive or negative) required by the load.

The direct parallel structure connect each source directly to the load. Due to the higher impedance of the FC compared to the one of SCs, this structure takes into account the natural constraints of each source. Moreover, it also establishes a favorable correlation between state of charge of SCs and instantaneous power load. Nevertheless, the FC specificities can not be fully insured due to the ohmic losses of SCs that induce partial transmission of current transient from the load to the FC. This can be only overcame by an overvalued capacity of the SCs.

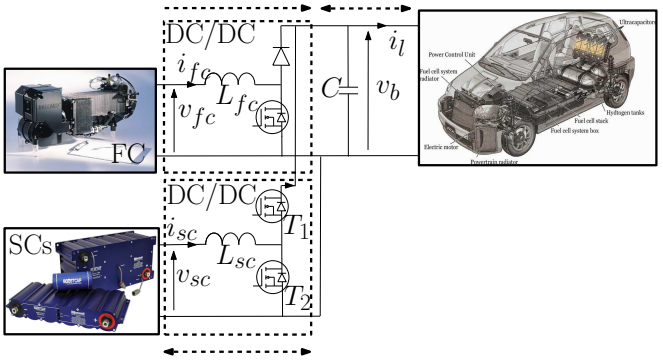

Fig. 1. Two converters parallel structure studied in this work.

The parallel structure with two converters (Fig. 1) associates with each source a static converter [6]. This architecture allows a perfect control of the power flow of each source. However, its drawbacks are the inevitable losses associated with each static converter and a higher cost. In particular, the power delivered by the permanent source (FC) is continually diminished by the losses of its converter.

The parallel structure with only one converter consists on the connection of the FC directly with the load, and uses a single “interface” converter to tune the power flow [7]. This converter is only used intermittently, since it ensures the adaptation of electrical voltage and current between the SCs and the load. Its main advantages are simplicity, losses reduction and costs related to interface power management.

These last two architectures can fully respect the mentioned requirements. This paper is dedicated to the study of the second structure shown in Fig. 1.

Given that high-performance controller are readily available [1], [6]–[8], where the SCs provide power transient, while the current delivered by the FC is slowly varying in order to ensure its live time. The controller adopted in [7] validates the described approach and demonstrates a better efficiency than unattended [8], unfortunatelly the closed-loop system stability is not theoretically proved.

Therefore, this drawback seems a theoretically challenging problem, while maintaining the same objectives and components security. Therefore, in this work a passivity-based controller has been studied in order to prove the global asymptotic stability of the closed-loop system. This non-linar controller is based on the well-known Interconnection and Damping Assignment - Passivity Based Control (IDA-PBC).

This paper is organized into three sections as follows : in section two, the paper describes some standard power management controllers based on a frequency decoupling of the sources. The proposed passivity-based controller is detailled in section three, and simulation results are presented in section four.

II. An overview a classical controllers

A first control strategy of the two converters structure has been detailed in [7]. It relies on the frequency decoupling of the sources (see Fig. 2) according to the power demands. The DC bus capacitor filters the high frequencies (i.e. above the kHz), the SCs associated with its converter provides the medium frequencies (from kHz to Hz) and the FC ensures the low frequencies (less than one Hz). This frequency decoupling of the sources naturally induces a power management strategy based on cascaded loops presented in Fig. 3.

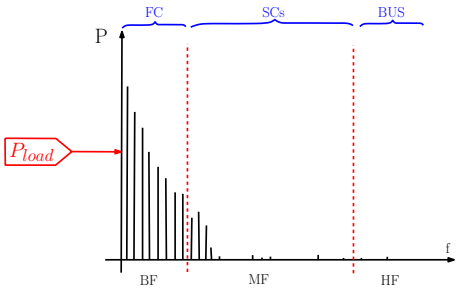

Fig. 2. Frequency decoupling principal.

Any power load modification induces a change in the DC bus voltage. It seems judicious to control the DC bus voltage with the SCs by computing the reference current i^*_{sc}, and thus regulate the bus voltage to its reference. Furthermore, the outer voltage loop associated with the SCs management must maintain the DC bus voltage at a constant reference v^*_b fixed at 50V.

On the other hand, the more faster the DC bus control is, the more smaller the capacity value of C is. The computed reference current i^*_{sc} must be lower in absolute value than the rated current $(|i_{sc}| < i_{rated})$, due to to heating and energy effectiveness. This is done by a signal issued by a

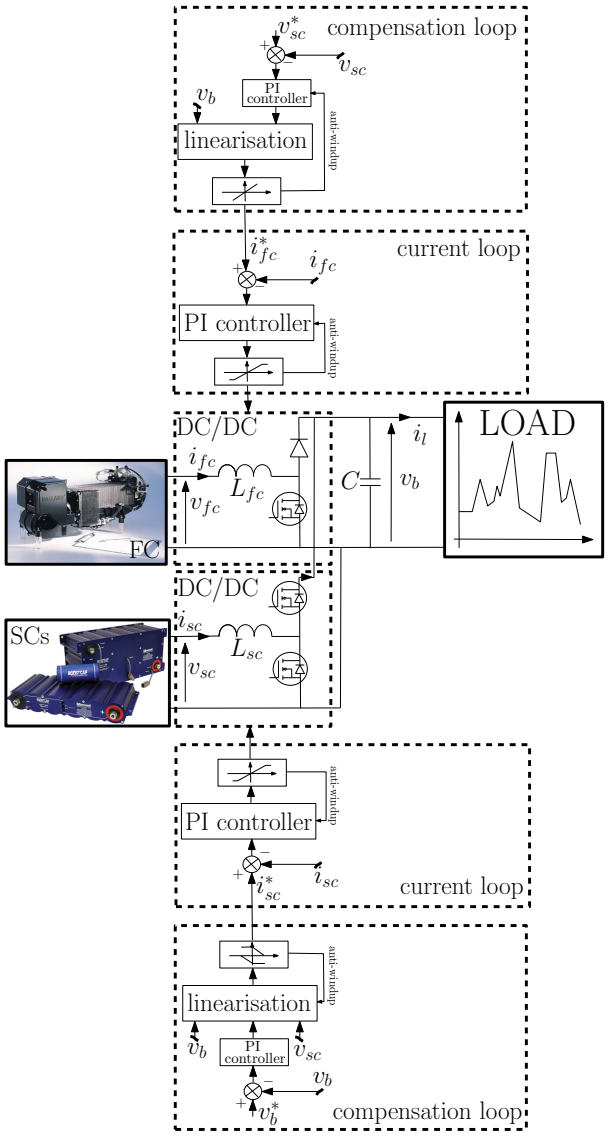

Fig. 3. Block diagram of first control-command management strategy.

saturation function which allows to maintain the SCs voltage v_{sc} in the interval $[(v_{sc})_{min}, (v_{sc})_{max}]$. The current loops are based on proportional-integral controller. Thus, the voltage closed-loop controller bandwidth is chosen ten time lower than the current closed-loop controller bandwidth. However, the SCs request for assistance would result in a permanent discharge of SCs, which would impose an excessive size of this latter to continuously provide and absorb power during fast transients. Therefore, the control system must maintain the SCs state of charge at a desired value. This can be ensured by a compensation loop whose purpose is to regulate the SCs voltage v_{sc} in their references v^*_{sc}.

The compensation controller is a proportional-integral controller. Thus, its bandwidth is chosen to meet the FC constraints, approximatively of one Hz. This frequency bandwidth is much lower than the current loops and the DC voltage bus bandwidths. Also, the compensation loop generates a current reference i^*_{fc} with a slow dynamic. This meets the frequency decoupling requirement and allows good control of the SCs to

their voltage reference levels.

The frequency decoupling adopted in [7] validates the described approach and demonstrates a better efficiency than unattended [8]. The SCs provide power transient, while the current delivered by the FC is slowly varying in order to ensure its longevity. The gains are tuned to ensure the closed loop system stability, although it is not theoretically proved.

Therefore, an alternative solution consists on developing a linear or non-linear controller with the same objectives and ensures the closed loop stability of the system. In this work, we developed a passivity-based controller for its many theoretical and practical advantages.

III. Passivity-based controller

A. Introduction

The second control strategy is based on passivity (PBC, Passivity-Based Control). The name "Passivity-Based Control" was introduced for the first time in [9] to define a design methodology that ensure stability of a non-linear system by making it passive. A non-linear system of the form :

$$\begin{array}{rcll} \dot{x} & = & f(x)+g(x)u; & x\in\Re^n; u\in\Re^m \\ y & = & h(x); & y\in\Re^m \end{array} \quad (1)$$

is said to be passive [10]–[12] over the supply rate function $s(u,y)=u^Ty$, if there exists a non-negative function C^0, called storage function $H:\Re^n\rightarrow\Re$, satisfying $H(0)=0$ and such that for all initial condition x_0, for all $t>0$ and any control input $u(.)$, the following inequality holds :

$$H(x(t))-H(x_0)\leq\int_0^t u^T(s)y(s)ds$$

"The amount of energy stored in a time interval is never greater than the total energy supplied during this period".

The immediate consequences of passivity are : if $u=0$ or $y=0$ then the energy function H is decreasing. So passive systems with a storage function H positive definite are stable in Lyapunov sense. Readers wishing to deepen this analysis can refer to [12] for further details.

B. Port controlled Hamiltonian system

The PBC defines a controller design methodology that stabilizes the system by making it passive. Specifically, this stabilizing effect is obtained by injecting the required damping in the system to bring an energy function to a minimum at the desired balance. Although there are many variations on this basic idea, the PBC can be broadly classified into two major groups. The "classical" PBC for which the designer chooses the storage function (usually quadratic), and then designs the controller that makes the storage function non-increasing.

In the second PBC methodology, the storage function of the closed loop system is left free, but the designer needed a control structure, such as Lagrangian or port-controller Hamiltonian (PCH), and then, he characterizes all assignable energy functions. This characterization is given in terms of solutions of partial differential equations (PDE). The most notable examples of this approach are the controlled Lagrangian systems, and the interconnexion and damping assignment - passivity based control (IDA-PBC) [13]. It is the latter method that is adopted in this work.

Firstly, the IDA-PBC approach consists on identifying the natural energy function of the system called $H(x)$, then rewrite the non-linear system (1) versus the gradient of the energy function :

$$\nabla H(x) \quad = \quad \left[\begin{array}{cccc} \frac{\partial H}{\partial x_1}(x) & \frac{\partial H}{\partial x_2}(x) & ... & \frac{\partial H}{\partial x_n}(x) \end{array}\right]^T$$

Thus, the PCH form of the initial system (1) is

$$\begin{array}{rcl} \dot{x} & = & [J(x)-\mathcal{R}(x)]\nabla H(x)+g(x)u \\ y & = & g^T\nabla H(x) \end{array} \quad (2)$$

where y is the output, $\mathcal{J}(x)=-\mathcal{J}^T(x)$ is a skew-symmetric matrix of dimension $n\times n$ representing the interconnections between states, and $\mathcal{R}(x)=\mathcal{R}^T(x)\geq 0$ is a positive semi-define symmetric matrix representing the natural damping of the system. The vectors u and $y\in\Re^m$ are conjugated variables whose product has units of power. The choice of PCH models was motivated by the fact that they are natural candidates to describe many physical systems.

Equation (2) shows that the PCH structure provides essential energy information for the design of the closed-loop system. Thus, the interconnection matrix $J(x)$ gives already an indication of the power exchange or balance between the variables, while the property of the positive semi-definite matrix $\mathcal{R}(x)$ indicates that the terms associated with this matrix represent the dissipation.

C. The IDA-PBC Methodology

Proposition 1 : Consider the system

$$\dot{x}=f(x)+g(x)u \quad (3)$$

assume there are matrices $g^\perp(x)$, $\mathcal{J}_d(x)=-\mathcal{J}_d^T(x)$, $\mathcal{R}_d(x)=\mathcal{R}_d^T(x)\geq 0$ and a function $H_d(x):\Re^n\longrightarrow\Re$ that verify the partial differential equation (PDE)

$$g^\perp(x)f(x)=g^\perp(x)[\mathcal{J}_d(x)-\mathcal{R}_d(x)]\nabla H_d \quad (4)$$

where $g^\perp(x)$ is a full-rank left annihilator of $g(x)$, that is, $g^\perp(x)g(x)=0$, and $H_d(x)$ is such that

$$\bar{x}=argmin(H_d(x)) \quad (5)$$

with $\bar{x}\in\Re^n$ the (locally) equilibrium to be stabilized. Then, the closed-loop system (3) with the control u, where

$$\begin{array}{rcl} u & = & \left[g^T(x)g(x)\right]^{-1}g^T(x) \\ & \times & \left\{[\mathcal{J}_d(x)-\mathcal{R}_d(x)]\nabla H_d-f(x)\right\} \end{array} \quad (6)$$

takes the PCH form

$$\dot{x}=[\mathcal{J}_d(x)-\mathcal{R}_d(x)]\nabla H_d \quad (7)$$

with $\bar{x}$ a (locally) stable equilibrium. It will be asymptotically stable if, in addition, $\bar{x}$ is an isolated minimum of $H_d(x)$ and the largest invariant set under the closed-loop dynamics (7) contained in

$$\left\{x\in\Re^n|\,[\nabla H_d]^T\,\mathcal{R}_d(x)\nabla H_d=0\right\} \quad (8)$$

equals $\bar{x}$. An estimate of its domain of attraction is given by the largest bounded level set $\{x \in \Re^n | H_d(x) \leq c\}$.

Proof : Setting up the right hand side of (3) equal to the right hand side of (7), we get the matching equation

$$f(x) + g(x)u = [\mathcal{J}_d(x) - \mathcal{R}_d(x)]\nabla H_d \tag{9}$$

Multiplying on the left by $g^{\perp}(x)$, we obtain the PDE (4). The expression of the control is obtained by multiplying on the left by the pseudo-inverse of $g(x)$. Stability of $\bar{x}$ is established noting that, along the trajectories of (7), we have

$$\dot{H}_d = -\left[\nabla H_d\right]^T \mathcal{R}_d(x) \nabla H_d \leq 0 \tag{10}$$

Hence, $H_d(x)$ is qualified as a Lyapunov function. Asymptotic stability follows immediately invoking the La Salle's invariance principle and the condition (8). Finally, to ensure that the solutions remain bounded, we give the estimate of the domain of attraction as the largest bounded level set of $H_d(x)$.

D. Design of the power flow controller

1) Controller structure: One solution to design the energy flow controller can be based on the full non-linear system (see as example [14]). However, such control does not give a safe control of the currents, inherent defect of state feedback controllers. Indeed, such control does not guarantee that the current i_k and i_{sc} are in a bandwith to protect the source, converters and the load.

Therefore, a classic solution consists on designing a cascaded control, as previously detailed in Section II. Fig. 4 represents the controller adopted in this work. It is composed of three subsystems : an inner current loop controller for the FC based on a PI controller, an inner current loop controller to manage the current of the SCs based on a PI controller, and only one outer loop to control the DC bus voltage and state of charge of the SCs.

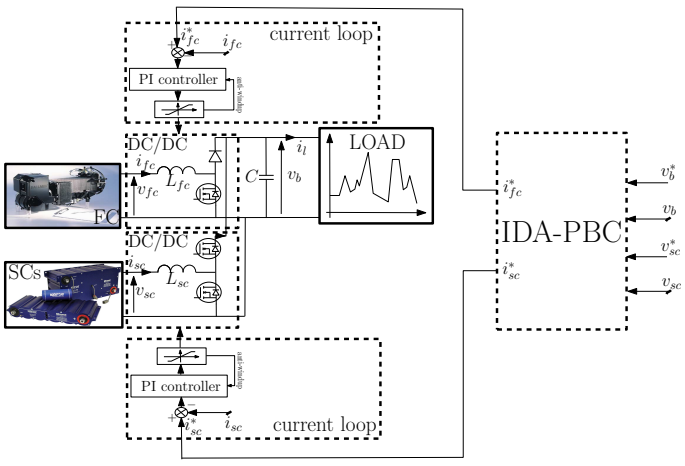

Fig. 4. IDA-PBC structure.

2) Hybrid system modeling: In this study, the modeling of the different elements is the same as in numerous studies [14], [15].

a) Fuel cell modeling: The model used is a static model, because the chemical reaction dynamic is faster than the electrical system dynamics. This voltage depends on the FC current density $j = i_{fc}/S$ (S = 110 cm^2 in the Ballard fuel cell), the hydrogen and oxygen partial pressure, the temperature and the membrane hydratation. The output voltage of a single cell v_{cell} and the FC voltage v_{fc} can be defined as follow :

$$\begin{array}{rcl} v_{cell} & = & E - v_{act} - v_{ohm} - v_{con} \\ v_{fc} & = & n\, v_{cell} \end{array} \tag{11}$$

where :

- E is the the thermodynamic potential of one cell ($\approx$ 1.031 V),
- v_{act} is the voltage drop due to the activation phenomena,
- v_{ohm} is the ohmic drop due to electronic and ionic internal resistances,
- v_{con} the voltage drop due to the limiting kinetics of gases throught the electrodes that appeared at high current density,
- n the number of cells.

and

$$\begin{array}{rcl} E & = & 1.229 - 8.5 \times 10^{-4} \left(T_{fc} - 298.15\right) \\ & + & 4.3085 \times 10^{-8}\, T_{fc} \left(ln(p_{H_2}) + \frac{1}{2} ln(p_{O_2})\right) \\ v_{act} & = & v_0 + v_1 \left(1 - e^{-c_1\, j}\right) \\ v_{ohm} & = & R_m\, j \\ v_{con} & = & j \left(c_2 \frac{j}{j_{max}}\right)^{c_3} \end{array} \tag{12}$$

where the fuel cell temperature T_{fc} is expressed in Kelvin, and the reactant partial pressures p_{H_2} and p_{O_2} are expressed in atm [16] (for more details see [17]).

Finally, the FC voltage v_{fc} is computed according to the current stack i_{fc} by a 5^{th} order polynomial function of the stack current i_{fc}, as shown in Fig. 5.

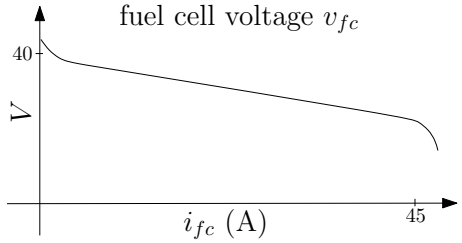

Fig. 5. Fuel cell voltage vs current.

b) Boost converter: To use the FC system in an electric power system, we must be able to connect the FC to a fixed DC bus voltage. In this case, we must increase the FC voltage, because it is often less than the DC bus voltage. The boost converter represented on the Fig. 6 have as control input the binary input $u_1(t)$. Defining α_1 as the duty cycle of the control variable $u_1(t)$, this subsystem can be represented by its average model (here, we considered that the switches are ideals) :

$$\frac{di_{fc}}{dt} = \frac{1}{L_{fc}} \big(-\left(1 - \alpha_1\right) v_b + v_{fc} \big) \tag{13}$$

The instantaneous model shows a non-linear behavior of the converter by the existence of products between the control α_1 and state variable v_b.

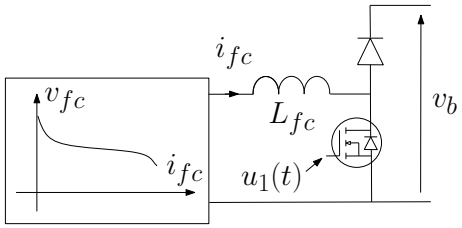

Fig. 6. Boost converter.

c) Buck-Boost Converter: The storage elements connection on the DC bus are done through static converters with reversible power, since SCs can be loaded or unloaded.

The SCs used here have a constant capacity C_{sc} and negligible losses. It is associated with an inductance L_{sc} and an elementary switching cell as shown in Fig. 7. This cell is bi-directional in current. Two types of operation are possible : a buck operating mode when SCs receive energy from the DC bus, and a boost operating mode when SCs provide energy to the DC bus.

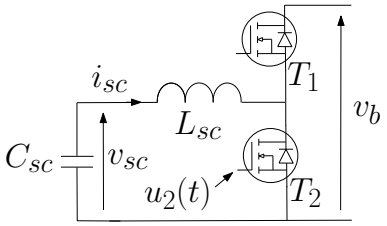

Fig. 7. Buck-boost converter.

We define α_2 the duty cycle of the control variable $u_2(t)$. The second sub-system is represented in the average sense by the two following equations:

$$\begin{array}{rcl} \frac{di_{sc}}{dt} & = & \frac{1}{L_{sc}}\big(-(1-\alpha_2)\,v_b + v_{sc}\big) \\ \frac{dv_{sc}}{dt} & = & -\frac{i_{sc}}{C_{sc}} \end{array} \tag{14}$$

d) DC bus and load model: The figure below shows the model of the DC bus and the load. In our work, the load is modeled by a $(R_l\, L_l)$ circuit, whose resistance value R_l varies depending on the power demanded by the load. The average model is:

$$\begin{array}{rcl} \frac{dv_b}{dt} & = & \frac{1}{C}\big((1-\alpha_1)\,i_{fc} + (1-\alpha_2)\,i_{sc} - i_l\big) \\ \frac{di_l}{dt} & = & \frac{1}{L_l}\big(-R_l i_l + v_b\big) \end{array} \tag{15}$$

e) Complete model: It follows that the complete system "fuel cell - supercapacitors" may be represented by the 5^{th} order non-linear state space model :

$$\begin{array}{rcl} \dot{x}_1 & = & \frac{(1-\alpha_1)\,x_4 + (1-\alpha_2)\,x_5 - x_3}{C} \\ \dot{x}_2 & = & -\frac{x_5}{C_{sc}} \\ \dot{x}_3 & = & \frac{-R_l\,x_3 + x_1}{L_l} \\ \dot{x}_4 & = & \frac{-(1-\alpha_1)\,x_1 + z}{L_{fc}} \\ \dot{x}_5 & = & \frac{-(1-\alpha_2)\,x_1 + x_2}{L_{sc}} \end{array} \tag{16}$$

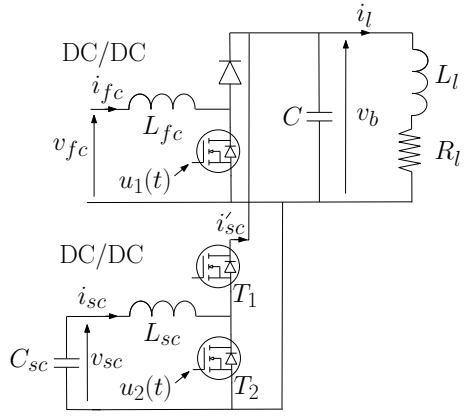

Fig. 8. DC bus and load model.

with the state space $x(t)$

$$x \;=\; [x_1;\, x_2;\, x_3;\, x_4;\, x_5]^t = [v_b;\, v_{sc};\, i_l;\, i_{fc};\, i_{sc}]^t \tag{17}$$

the control inputs $u(t) = [u_1;\, u_2]^t = [1-\alpha_1;\, 1-\alpha_2]^t$, the measures $y(t) = x$ and $z(t) = v_{fc}$.

3) Outer closed loop control: The currents control is provided by two fast inner loops, so we can assume that the currents are equal to their references according to the voltage time scale. Under these conditions, the 5^{th} order system can be reduced to a 3^{th} order system, whose state equation is given below :

$$\begin{array}{rcl} \dot{x}_1 & = & \frac{1}{C}\big(\frac{z_3}{x_1}\,u_1 + \frac{x_2}{x_1}\,u_2 - x_3\big) \\ \dot{x}_2 & = & -\frac{u_2}{C_{sc}} \\ \dot{x}_3 & = & \frac{-R_l\,x_3 + x_1}{L_l} \end{array} \tag{18}$$

with

$$x = [x_1;\, x_2;\, x_3]^t \;=\; [v_b;\, v_{sc};\, i_l]^t; \tag{19}$$

the control inputs $u = [u_1;\, u_2]^t = [i_{fc};\, i_{sc}]^t$ and the measures $y = [v_b;\, v_{sc};\, i_l]^t$ and $z = [i_{fc};\, i_{sc};\, v_{fc}]^t$, with the desired equilibrium point $\bar{x} = [\bar{x}_1;\, \bar{x}_2;\, \bar{x}_3] = [v_b^*;\, v_{sc}^*;\, \frac{v_b^*}{R_l}]$, with v_b^* and v_{sc}^* the DC bus and SCs desired voltages, and the storage function $H(x) = \frac{1}{2}x^t Q x$ with $Q = diag(C;\, C_{sc};\, L_l)$.

4) PCH model of the outer loop control: We look for an energy function $H(x)$ so that its minimum is reached at the desired equilibrium point $\bar{x}$. Also, a choice of the energy function H is :

$$H_d = \frac{1}{2}\,\tilde{x}^t\,Q\,\tilde{x} \quad \text{with} \quad \tilde{x} = x - \bar{x} \tag{20}$$

In these circumstances, writing the PCH system (2) in terms of the dynamics of the error and the gradient of the closed-loop desired energy function ∇H_d is:

$$\dot{\tilde{x}} = [J - \mathcal{R}]\nabla H_d + A(u, \bar{x}) \tag{21}$$

with

$$J - \mathcal{R} = \begin{bmatrix} 0 & 0 & -\frac{1}{L_l\,C} \\ 0 & 0 & 0 \\ \frac{1}{L_l\,C} & 0 & -\frac{R_l}{L_l^2} \end{bmatrix} \tag{22}$$

$$\begin{aligned} \nabla H_d &= \left[\, C\,\tilde{x}_1; C_{sc}\,\tilde{x}_2; L_l\,\tilde{x}_3 \,\right]^t \\ A(u,x,\bar{x},z) &= \begin{bmatrix} \frac{1}{C}\left(\frac{z_3}{x_1}\,u_1 + \frac{x_2}{x_1}\,u_2 - \bar{x}_3\right) \\ -\frac{1}{C_{sc}}\,u_2 \\ 0 \end{bmatrix} \end{aligned} \quad (23)$$

5) IDA-PBC controller equation: The following control laws are proposed :

$$\begin{aligned} u_1 &= \frac{x_1}{z_3}\left(\frac{\bar{x}_1}{R_l} - r_1\,\tilde{x}_2\right); \qquad r_1 > 0 \\ u_2 &= -r_1\,\tilde{x}_1 \end{aligned} \quad (24)$$

so that the closed-loop system is as follows:

$$\dot{\tilde{x}} = [J_d - \mathcal{R}_d]\nabla H_d \quad (25)$$

with

$$J_d = \begin{bmatrix} 0 & -\frac{r_1}{C\,C_{sc}} & -\frac{1}{L_l\,C} \\ \frac{r_1}{C\,C_{sc}} & 0 & 0 \\ \frac{1}{L_l\,C} & 0 & 0 \end{bmatrix}, \mathcal{R}_d = \begin{bmatrix} \frac{x_2\,r_1}{x_1\,C^2} & 0 & 0 \\ 0 & 0 & 0 \\ 0 & 0 & \frac{R_l}{L_l^2} \end{bmatrix} \quad (26)$$

The proof of asymptotic stability is deduced from the derivative analysis of H_d :

$$\dot{H}_d = \nabla H_d^t\,\dot{\tilde{x}} = -\nabla H_d^t\,R_d\,\nabla H_d^t \leq 0 \quad (27)$$

and the invariance principle of the LaSalle theorem with $H_d(\bar{x}) = \dot{H}_d(\bar{x}) = 0$. Moreover, H_d is radially unbounded, therefore the closed-loop system is globally asymptotically stable.

The control equation analysis shows that SCs provide the energy due to an error on the DC bus voltage, the error itself is caused by power spikes or a variation of the DC bus voltage reference. The desired current i_{fc}^* shows that the FC provides two main objectives :

- the permanent power flow from the FC to the load,
- the energy contribution to regulate the SCs voltage.

Compared to the first controller, the number of degrees of freedom is equal to one parameter, so that the matrix $J(x)$ is an skew symmetric matrix. This can be seen as a weakness of this command.

IV. Simulation and Experimental Results

In this section, we present simulation results of two cases. We notice that for the implementation of the proposed controller the knowledge of the load resistance R_l is needed for the computation of the FC reference current. To explain the rational of the design procedure, first, we consider the case when the load resistance R_l is known. An integral action or load resistance observer scheme is later added in the second case studied.

A. The known parameter case

Fig. 9 represents the *scenarii* of all the simulations composed of two stages :

- a variation of the reference DC bus voltage with a constant load ($R_l = 10\Omega$) between times 0 and 16s,
- then a variation of the load equal to 100% with a DC bus voltage constant at time 16s.

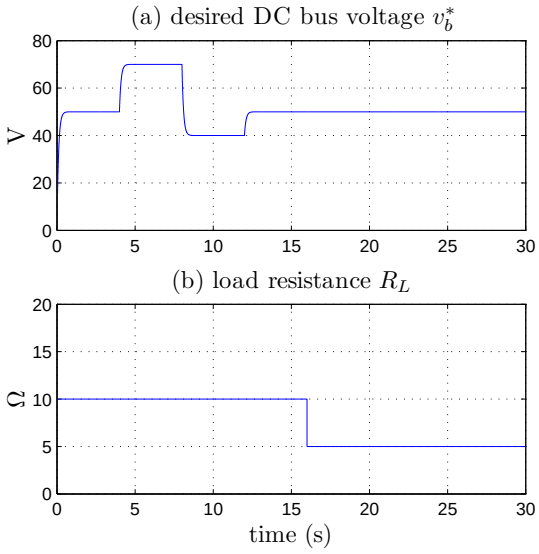

Fig. 9. *scenarii.*

Fig. 10 represents the response of the hybrid system with the *scenarii*, and shows that the command ensures perfect control of the DC bus voltage, the SCs respond rapidly to fast current transient to provide most of the power required by the load and to maintain the DC bus voltage at its reference value.

This allows the FC to have a smooth response during fast power demand of the load (10.e), what improves his state of health. Then gradually with the FC current increasement, the SCs discharge, characterized by the decrease of its voltage, vanishes to zero (10.b, 10.e).

B. The unknown parameter case

a) Introduction: However, in practice the load resistance is not know. Therefore, in the case of a load power increase, the FC current is not enougth high and consequently the SCs voltage is not regulated to the reference value equal to 12V. Fig. 11 represents the response of the hybrid system in a such case, where the load resistance is supposed equal to $10\,\Omega$. Between time 16 and 20s, the SCs does not recover the equilibrium and under these conditions, SCs provide too much energy during the power transition and SCs recharging is uncertain.

To remedy to this problem, two solutions are explored. In the first one, a low integrator action is added to the command $u_1 = i_{fc}^*$, while in the second approach, an estimate of the load resistance eliminates this error.

b) IDA-PBC controller + integral action: The controller design supposed that the converters are loss-less. So in practice, a low integrator action need to be added to the passivity controller in order to insure zero voltage error at steady state and to counteract the unknow load resistance involvement. The controller equation is now :

$$\begin{aligned} \dot{x}_c &= \gamma\,\tilde{x}_2 \\ u_1 &= \frac{x_1}{z_3}\left(\frac{\bar{x}_1}{R_l} - r_1\,\tilde{x}_2\right) - x_c; \qquad r_1 > 0 \\ u_2 &= -r_1\,\tilde{x}_1 \end{aligned} \quad (28)$$

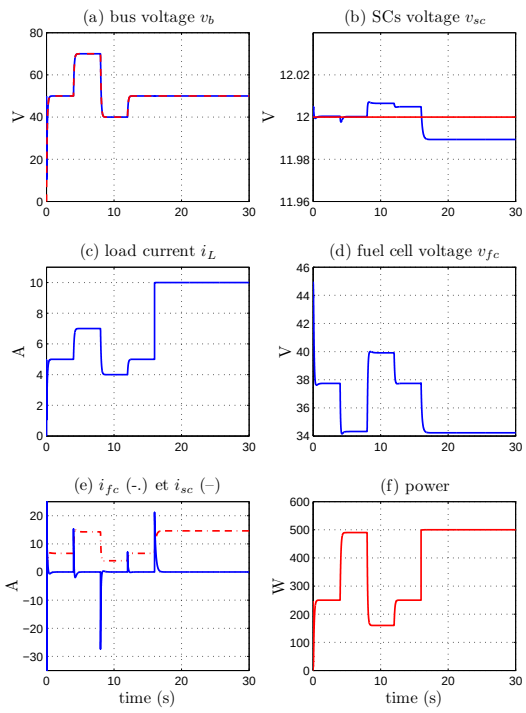

Fig. 10. Simulation result with the resistance as known parameter (r_1=100).

Fig. 12 shows the system response. It is observed that the DC bus and SCs voltages reached the desired equilibrium point. Then, it's established a balance of energy, characterized by a charge of SCs to their desired value set at 12V.

c) IDA-PBC controller + load resistance observer: In practical applications the load resistance is, of course, unknown, and we propose to estimate it using a nonlinear observer as shown in Fig. 13. The non-linear state space model of the observer is as follow :

$$\begin{aligned} \dot{\hat{x}} &= \begin{bmatrix} -\frac{1}{L_l}\hat{x}_1\,\hat{x}_2 \\ 0 \end{bmatrix} + \frac{1}{L_l}\begin{bmatrix} 1 \\ 0 \end{bmatrix} u + \begin{bmatrix} k_1 \\ k_2 \end{bmatrix}(\hat{y}-y) \\ \hat{y} &= \begin{bmatrix} 1 & 0 \end{bmatrix}\hat{x} \end{aligned} \tag{29}$$

where the state space $\hat{x}(t)$ is $[\hat{x}_1;\,\hat{x}_2]^t = [\hat{i}_l;\,\hat{R}_l]^t$, the control inputs $u(t)$ is the DC bus voltage v_b, the load current measurement i_l as mesure $y(t)$, and k_1 and k_2 are some positive design parameters. Here, the evolution of the load resistance is not know, for that reason we supposed that R_l is nearly constant between two time sample, i.e. $\frac{d}{dt}R_l = 0$ in continuous time or $R_l[k] = R_l[k-1]$ in discret time.

Fig. 14 and 15 show respectevely the observer behaviour where the load resistance change are well estimated, and the complet system performances when the load resistance estimate is used in the controller. The last figure shows that the controller associated with the observer leads to an nearly zero static error of the SCs voltage at steady state without adding an integral action. Nevertheless, a low intagral action need to be added in a pratical application to compensate for

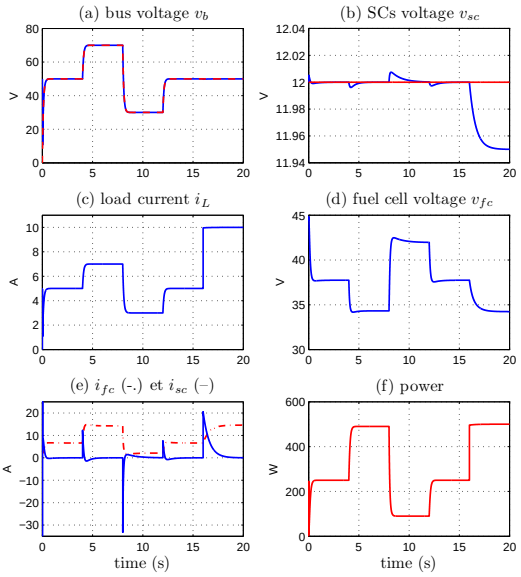

Fig. 11. Simulation result with the resistance as unknown parameter (r_1=100).

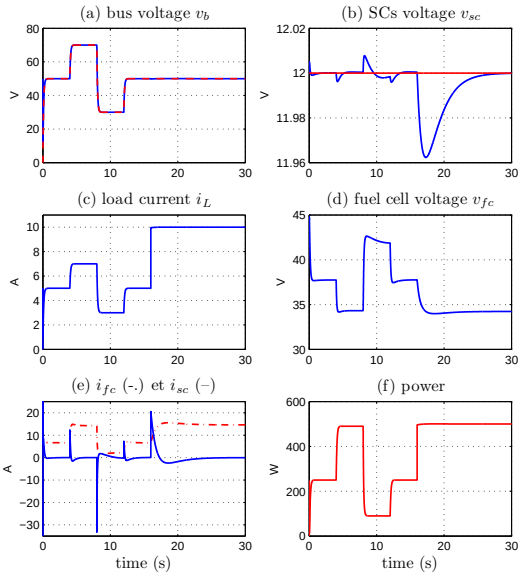

Fig. 12. Simulation result with an integral action (r_1=100, γ=50).

the converter losses.

Proof of the global stability of the system : The proof of the global stability of the system composed of the controller, the observer and electrical system is established invoking a theorem on stability of cascaded systems stated in [18].

Proposition 2 : Consider the hybrid system (18) in closed-loop with the control law (24) where R_l is replaced by $\hat{R}_l$ generated by (29). We have that $lim_{t\longrightarrow\infty}x(t) = \bar{x}$ for all initial conditions.

Proof : Let us define the estimation error $\tilde{\tau}_l = \hat{R}_l - R_l$, and write the closed-loop system in the following form:

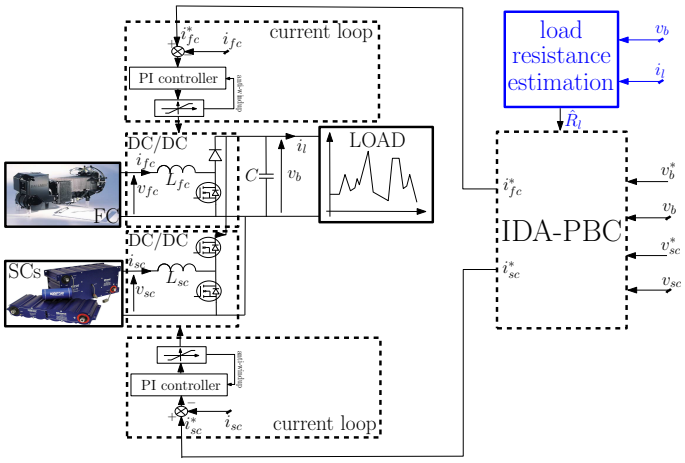

Fig. 13. IDA-PBC structure with the load resistance observer.

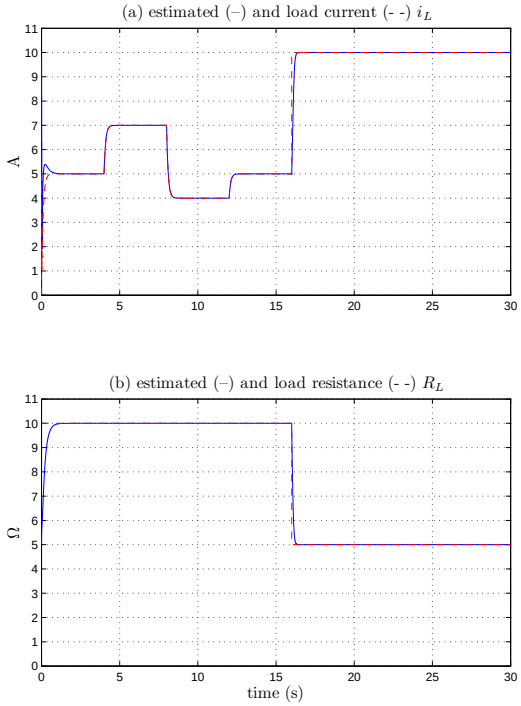

Fig. 14. Observer behaviour (k_1=50, k_2=10).

$$\dot{\tilde{x}} = [\mathcal{J}_d(x) - \mathcal{R}_d(x)]\nabla H_d(x) + \varphi(x)\tilde{R}_l \qquad (30)$$

with $\varphi(x) = \begin{bmatrix} \frac{\bar{x}_1}{C} \\ 0 \\ 0 \end{bmatrix}$

To prove the stability of the closed-loop non-linear estimator (29), consider the Lyapunov function :

$$V = \frac{1}{2}\tilde{x}^t\,\tilde{x} \qquad (31)$$

with

$$\begin{bmatrix} \dot{\tilde{x}}_1 \\ \dot{\tilde{x}}_2 \end{bmatrix} = \begin{bmatrix} -\frac{1}{L_l}(x_1\tilde{x}_2 + x_2\tilde{x}_1 + \tilde{x}_1\tilde{x}_2) + k_1\tilde{x}_1 \\ k_2\tilde{x}_1 \end{bmatrix} \qquad (32)$$

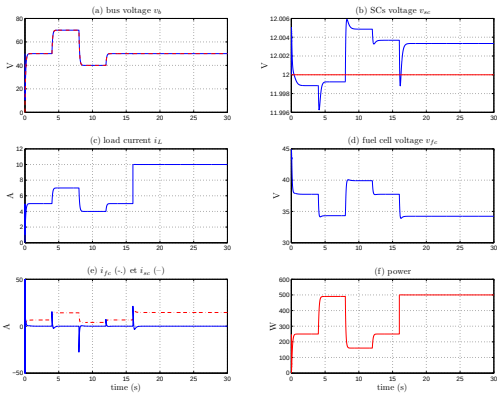

Fig. 15. Simulation with the load reistance observer(r_1=100, k_1=50, k_2=10).

The time derivative along the trajectories (32) is given by :

$$\begin{aligned} \dot{V} &= \tilde{x}_1\dot{\tilde{x}}_1 + \tilde{x}_2\dot{\tilde{x}}_2 \\ &= \tilde{x}_1^2(k_1 - \tfrac{\tilde{x}_2+x_2}{L_l}) + \tilde{x}_1\tilde{x}_2(k_2 - \tfrac{x_1}{L_l}) \end{aligned} \qquad (33)$$

which is negative if the two above properties are satisfied :

$$\begin{aligned} k_1 &< \tfrac{\tilde{x}_2+x_2}{L_l} \\ k_2 &= \tfrac{x_1}{L_l} - k\,\tfrac{\tilde{x}_2}{\tilde{x}_1} \qquad \text{with} \quad k>0 \end{aligned} \qquad (34)$$

This is an autonomous non-linear system, which is asymptotically stable for all positive gains k_1 and k_2 that satisfied the two properties (34). Thus, the estimation errors decay asymptotiquement to zero.

The overall error dynamics is a cascade composition like the ones studied in [[18],Th.2], whose conditions we will now verify. First, the nominal part of the first subsystem (30), namely $\dot{\tilde{x}} = [\mathcal{J}_d(x) - \mathcal{R}_d(x)]\nabla H_d(x)$, is globally asymptotically stable. Further, the Lyapunov function H_d is a quadratic function, thus it satisfies the bounds

$$\begin{aligned} \left\|\tfrac{\partial H_d}{\partial x}(x)\right\|\|x\| \le c_1 H_d(x), \qquad & \forall\,\|x\| \ge \eta \\ \left\|\tfrac{\partial H_d}{\partial x}(x)\right\| \le c_2, \qquad & \forall\,\|x\| \le \eta \end{aligned}$$

where $c_1, c_2, \eta > 0$.This is condition (A.1) of [[18],Th.1]. Second, from inspection of the definitions of $\varphi(x)$ above, and the fact that $\tilde{R}_l$ is bounded, we have that the interconnection term satisfies the bound

$$\|\varphi(x)\| \le c_3 + c_4\,|x_3|$$

for some $c_3, c_4 > 0$, as required by condition (A.2). Finally, the last condition of the theorem, requiring that the second subsystem in (30) be globally uniformly asymptotically stable and that its response to initial condition be absolutely integrable, is satisfied since the subsystem (29) is asymptotiquement stable. This completes the proof of our proposition.

C. Experimental results

V. Conclusion

In this paper, a new control strategy to ensure energy management between two energy sources, namely a hydrogen

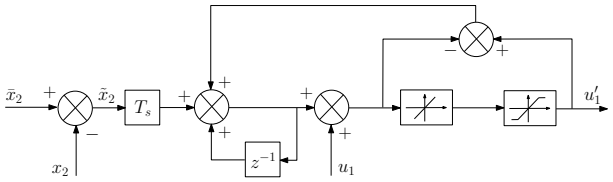

Fig. 16. FC current limitation

fuel cell and supercapacitors is discussed. This new control law based on passivity ensures global asymptotic stability of the closed loop system, while reducing the load stress on the stack power transients. The simulation results show good behavior to the load stress. In addition, this controller has a single tuning parameter, which gives an ease of implementation on a real-time system.

However, the controller design pre-supposes that the load resistance is well-know. In this work, an integrator has been added to compensate this drawback.

REFERENCES

[1] Thounthong P., Raël S., Davat B., "Energy management of fuel cell/battery/supercapacitor hybrid power source for vehicle applications," *Journal of Power Sources*, Vol. 193, Issue 1, pp. 376-385, Agu. 2009.

[2] Corbo P., Migliardinia F., Veneri O. ,"PEFC stacks as power sources for hybrid propulsion systems," *International Journal of Hydrogen Energy*, Vol. 34, Issue 10, pp. 4635-4644, May 2009

[3] Giulii F., Cacciato M., "Using Super Capacitors in combination with Bi-Directional DC/DC Converters for Active Load. Management in Residential Fuel Cell Applications," *1st European. Symposium on Supercapacitors, IEEE-ESSCAP'04*, 2004.

[4] Cacciato M., F. Caricchi, Giuhlii F., Santini E., "A critical evaluation and design of bi-directional DC/DC converters for supercapacitors interfacing in fuel cell applications," *IEEE Industry Applications Conf., IEEE IAS'04*, Vol.2, pp. 1127-1133, Oct. 2004.

[5] Jiang Z., Gao L., Blackwelder M.J., Dougal R.A., "Design and experimental tests of control strategies for active hybrid fuel cell/battery power sources," *J. Power Sources*, Vol.130, pp. 163-171, 2004.

[6] Tounthong P., Raël S., Davat B., "Supercapacitors as an energy storage for fuel cell automotive hybrid electrical system," *International Journal of Electrical Engineering in Transportation*, Vol.1, No.1, 2005.

TABLE I

ELECTRIC CHARACTERISTICS OF THE HYBRID SYSTEM.

Fuel cell parameters	Value
Open circuit voltage E	45 V
Rated voltage	26 V
Rated current	46 A
Supercapacitors parameters	
Capacitance	125 F
Rated voltage	30 V
Rated current	200 A
Optimal voltage (v_{sc}^*)	24 V
Electric load parameters	
Rated power	1800 W
Rated voltage	60 V
Rated current	150 A
Inductance and capacitie parameters	
L_{fc} inductance	200 μH
L_{sc} inductance	100 μH
Rated current L_{fc}	100 A
Rated current L_{sc}	150 A
Capacities C	14 mF
Optimal DC bus voltage (v_b^*)	48 V

[7] Azib T., Bethoux O., Remy G., Marchand C., "Structure and Control Strategy for a Parallel Hybrid Fuel Cell/Supercapacitors Power Source," *IEEE VPPC'09* in Dearborn, Michigan, Sept 7-11. 2009.

[8] Azib T., Bethoux O., Marchand C., Berthelot E., "Supercapacitors for Power Assistance in Hybrid Power Source with Fuel Cell," *IEEE Industrial Electronics Society Conference IECON'09*, Porto, Portugal, 2009.

[9] R. Ortega, M. Spong, "Adaptive motion control of rigid robots : A tutorial," *Automatica*, 25(6), pp. 877-888, 1989.

[10] C. Byrnes, A. Isidori, J.C. Willems, "Passivity, feedback equivalence, and the global stabilization of minimum phase nonlinear systems," *IEEE Trans. on Automat. Contr*, volume 36(11), pp. 1228-1240, 1991.

[11] A.J. van der Schaft, "L2-Gain and Passivity Techniques in Nonlinear Control," *Springer-Verlag*, Berlin, 1996.

[12] R. Ortega, A. Loria, P.J. Nicklasson, H. Sira-Ramirez, "Passivity-based control of Euler-Lagrange systems," *Springer-Verlag*, Berlin, 1998.

[13] R. Ortega, A. van der Schaft, B. Maschke, G. Escobar, "Interconnection and damping assignment passivity-based control of port-controlled Hamiltonian systems," *Automatica*, 38(4), pp. 585-596, 2002.

[14] M. Becherif, "Passivity-based control of hybrid sources : fuel cell and battery," 11^{th} *IFAC Symposium on Control in Transportation Systems*, The Netherlands, 2006.

[15] S. Caux, J. Lachaize, M. Fadel, P. Shott, L. Nicod, "Modelling and control of a Fuel Cell System and Storage Elements in transport applications," *Elsevier, Journal of Process Control*, Vol. 15, pp.481-491, 2005.

[16] J.C. Amphlett, R.M. Baumert, R.F. Mann, B.A. Peppley, P.R. Roberge, "Performance modeling of the Ballard Mark IV solid polymer electrolyte fuel cell," *Jounal of Electrochemical*, 142(1), pp. 9-15, 1995.

[17] J.T. Pukrushpan, H. Peng, A.G. Stefanopoulou, "control-oriented modeling and analysis for automotive fuel cell systems," *Transactions on ASME*, Vol. 26, pp. 14-25, Mar. 2004.

[18] E. Panteley and A. Loria, "On global uniform asymptotic stability of nonlinear time varying systems in cascade," *Syst. Contr. Lett*, Vol. 33, no. 2, pp 131-138, Feb. 1998.